The EMBO Journal (2012) 31, 95–109 | © 2012 European Molecular Biology Organization | All Rights Reserved 0261-4189/12
www.embojournal.org

THE EMBO JOURNAL

Physical and functional interaction between PML and TBX2 in the establishment of cellular senescence

Nadine Martin[1,2,4,5], Moussa Benhamed[1,2,5], Karim Nacerddine[1,2,3], Maud D Demarque[1,2], Maarten van Lohuizen[3], Anne Dejean[1,2,*] and Oliver Bischof[1,2]

[1]Department of Cell Biology and Infection, Nuclear Organisation and Oncogenesis Laboratory, Institut Pasteur, Paris, France, [2]INSERM, U993, Paris, France and [3]Division of Molecular Genetics and The Centre of Biomedical Genetics, Academic Medical Center and Cancer Genomics Centre, Netherlands Cancer Institute, Amsterdam, The Netherlands

Cellular senescence acts as a potent barrier for tumour initiation and progression. Previous studies showed that the PML tumour suppressor promotes senescence, although the precise mechanisms remain to be elucidated. Combining gene expression profiling with chromatin-binding analyses and promoter reporter studies, we identify TBX2, a T-box transcription factor frequently overexpressed in cancer, as a novel and direct PML-repressible E2F-target gene in senescence but not quiescence. Recruitment of PML to the TBX2 promoter is dependent on a functional p130/E2F4 repressor complex ultimately implementing a transcriptionally inactive chromatin environment at the TBX2 promoter. TBX2 repression actively contributes to senescence induction as cells depleted for TBX2 trigger PML pro-senescence function(s) and enter senescence. Reciprocally, elevated TBX2 levels antagonize PML pro-senescence function through direct protein–protein interaction. Collectively, our findings indicate that PML and TBX2 act in an auto-regulatory loop to control the effective execution of the senescence program.

The EMBO Journal (2012) **31,** 95–109. doi:10.1038/emboj.2011.370; Published online 14 October 2011
Subject Categories: signal transduction; molecular biology of disease
Keywords: cellular senescence; chromatin; gene repression; PML; TBX2

Introduction

Cellular senescence represents a robust and essentially irreversible tumour-suppressive barrier that cells must overcome to develop into a full-blown malignancy, and is thus clearly distinguished from the reversible cell-cycle arrest of quiescence. Senescence is induced by telomere shortening (known as replicative senescence) or when cells face potentially cancer-causing events including tumour suppressor loss (e.g., PTEN) or oncogenic hyperactivation (e.g., oncogenic Ras^{V12} and $BRAF^{600E}$). Irrespective of the initial signal, senescence is characterized by a proliferative arrest as well as important changes in cytomorphology, metabolism (e.g., increased senescence-associated β-galactosidase activity, SA-β-Gal) and chromatin organization. The senescence response is a highly coordinated, genetically driven process that is regulated and executed by a tightly interwoven tumour suppressor network presided by the master tumour suppressors p53 and Rb (Campisi and d'Adda di Fagagna, 2007). The Rb family of proteins consists of three family members Rb1/p105, RbL1/p107 and RbL2/p130 (herein referred to as Rb, p107 and p130). All three are involved in the transcriptional repression of E2F-responsive target genes (Frolov and Dyson, 2004) and have overlapping as well as compensatory functions depending on cell and promoter context (Jackson and Pereira-Smith, 2006; Chicas *et al*, 2010). While Rb predominantly associates with transcriptional transactivators E2F1–3, p107 and p130 specifically bind transcriptional repressors E2F4–5 (Dyson, 1998; Takahashi *et al*, 2000; Trimarchi and Lees, 2002; Cam *et al*, 2004). In contrast to Rb, expression levels of p130 are cell cycle regulated and p130 is the most abundant Rb-family member in quiescent cells, where it is the only active Rb protein. While Rb function in senescence is well established much less is known about the role of p130 in this process (Helmbold *et al*, 2006).

Another tumour suppressor protein that is frequently found lost or mutated in cancers is the promyelocytic protein PML (Bernardi and Pandolfi, 2007). PML exists in seven major isoforms, designated PML I–VII, which are generated by alternative splicing (Jensen *et al*, 2001). The function(s) of these isoforms have remained by-and-large unexplored. PML I–VI are localized in the nucleoplasm and mostly concentrate into discrete subnuclear organelles termed PML nuclear bodies (NBs; Bernardi and Pandolfi, 2007). Nucleoplasmic PML and PML NBs have been linked to diverse biological processes including transcriptional regulation, but, to date, only very few direct target genes have been identified (Wang *et al*, 2004; Xu *et al*, 2004; Kumar *et al*, 2007). The PML protein was found to play an instrumental role in the establishment of cellular senescence both in primary human and in mouse embryonic fibroblasts (MEFs; Ferbeyre *et al*, 2000; Pearson *et al*, 2000). We have shown recently that among the several PML isoforms, PML-IV is the only one to induce senescence (Ferbeyre *et al*, 2000; Pearson *et al*, 2000; Bischof *et al*, 2002). While overexpression of PML-IV is sufficient to induce senescence in a p53/Rb-dependent fashion in human and murine embryonic fibroblasts, cells lacking

*Corresponding author. Department of Cell Biology, Nuclear Organisation and Oncogenesis Laboratory, Institut Pasteur, 28 rue du Dr Roux, 75724 Paris Cedex 15, France. Tel.: +33 1 40 61 33 07; Fax: +33 1 45 68 89 43; E-mail: adejean@pasteur.fr
[4]Present address: Cell Proliferation Group, MRC Clinical Sciences Centre, Imperial College Faculty of Medicine, Hammersmith, Hospital Campus, Du Cane Road, London W12 0NN, UK
[5]These authors contributed equally to this work

Received: 27 January 2011; accepted: 19 September 2011; published online: 14 October 2011

©2012 European Molecular Biology Organization

PML exhibit a reduced propensity to undergo senescence (Pearson *et al*, 2000; de Stanchina *et al*, 2004). Little is known about how PML-IV pro-senescence function is regulated. PML-IV acts in a positive feedback loop with p53 to induce senescence (de Stanchina *et al*, 2004) and the high-risk human papilloma viral oncoprotein E7 circumvents PML-IV-induced senescence by disrupting a PML–p53–CBP pro-senescent trimeric complex and Rb/E2F corepressor complexes (Mallette *et al*, 2004; Bischof *et al*, 2005). Recently, it was also demonstrated that PML is involved in senescence-associated repression of E2F-target genes through recruitment of E2Fs to PML NBs (Vernier *et al*, 2011).

The T-box protein 2 (TBX2) is a family member of transcription factors characterized by a highly conserved DNA-binding T-box domain (TB). TBX2 is structurally and functionally related to TBX3 and both have been implicated in cell-cycle control and oncogenesis. Excessive TBX2 and TBX3 (TBX2/3) protein levels facilitate immortalization of murine cells, cooperate with oncogenes in cellular transformation and delay senescence onset in primary human fibroblasts (Abrahams *et al*, 2010). The pro-proliferative and anti-senescence functions of TBX2/3 are best understood in murine cells where they have been shown to mediate transcriptional repression of $p15^{INK4B}$, $p16^{INK4A}$, $p21^{CIP}$ and $p19^{ARF}$ (p14 in human) tumour suppressors (Jacobs *et al*, 2000; Prince *et al*, 2004). Dysregulation of these genes invariably leads to compromised p53 and Rb tumour suppressor pathway functions. The TBX2 domains responsible for transcriptional repression have been mapped to the TB and a C-terminal conserved repression domains (RD1) (He *et al*, 1999; Jacobs *et al*, 2000; Lingbeek *et al*, 2002). In addition to antagonizing senescence, TBX2 may contribute to cancer progression by promoting polyploidy and resistance to the anti-cancer drug cisplatin (Davis *et al*, 2008) as well as anchorage-independent growth and survival (Ismail and Bateman, 2009). In line with its oncogenic function, TBX2 is frequently overexpressed in a number of cancers including breast, pancreatic and skin cancers (Abrahams *et al*, 2010). Induction of senescence by a dominant-negative form of TBX2 in murine B16 melanoma cells indicated an active contribution of this protein in cancerogenesis (Vance *et al*, 2005). Despite the data reported, little is still known about the anti-senescence functions of TBX2 in human cells and how TBX2 expression is regulated during senescence and after oncogenic insults.

To better understand the role PML plays in senescence, we sought to identify PML-target genes. Using gene expression profiling combined with chromatin immunoprecipitation (ChIP) and promoter reporter studies, we identify TBX2 as a novel PML-repressed E2F-target gene in senescence. Recruitment of PML to the TBX2 promoter is dependent on a functional p130/E2F4 repressor complex and coincides with the induction of an inactive chromatin state at the TBX2 promoter. Importantly, we find that PML and TBX2 physically interact in proliferating cells and that TBX2 overexpression ablates PML-induced senescence through direct protein–protein interaction. Depletion of TBX2 from proliferating cells induces senescence, indicating that senescence-associated TBX2 repression actively contributes to the execution of the senescence process, which is, at least in part, mediated by the activation of PML pro-senescence activity due to its release from the inhibitory effect of TBX2. Finally, PML-mediated TBX2 repression is independent from the integrity of PML NBs and specific for senescent cells, as it does not occur in quiescent cells. Although TBX2 is also repressed in quiescent cells PML is not involved in this repression, indicating that PML is uniquely required for the permanent repression of TBX2 in senescence opposed to the reversible repression in quiescence. Collectively, these data establish an important functional and physical link between PML and TBX2 in the implementation of the senescence state.

Results

TBX2 repression actively contributes to the senescence phenotype

To identify genes associated with the senescence program elicited by PML, we used high-density (Affymetrix U133A) oligonucleotide microarrays to generate gene expression profiles of pre-senescent and senescent WI38 primary human diploid fibroblasts (HDFs). Senescence of HDFs was induced either by introduction of PML-IV or Ras^{V12} using retroviral-mediated gene transfer into early passage WI38 cell populations or by replicative exhaustion of these cell populations by serial passaging. To detect changes in transcript abundance that are causative for the PML-induced senescence phenotype rather than a mere consequence of it, and to facilitate identification of genes that are subject to PML-mediated gene regulation, we decided to score for early rather than late transcriptional changes elicited by PML during the senescence process. Accordingly, PML-infected cells were recovered and total RNA prepared for cDNA microarray analysis 2 days post-selection (i.e., 4 days post-infection) at a time when the cells already began to cease proliferation (Supplementary Figure S1A). Ras^{V12}-induced senescent cells were analysed 8 days post-infection, at which time they were fully senescent as determined by SA-β-Gal staining and absence of BrdU incorporation (Bischof *et al*, 2002). In parallel, a culture of WI38 cells was infected with a control 'empty' vector and cells were recovered for analysis either at their point of exponential proliferation (i.e., pre-senescence, PS) or replicative senescence (RS). A number of genes have been shown to promote senescence upon loss of function including NF1, PTEN or BMI-1 (Jacobs *et al*, 1999; Chen *et al*, 2005; Courtois-Cox *et al*, 2006); therefore, we decided to focus on genes with decreased expression to study their importance for the senescence program. An one sample *t*-test comparing transcript abundance levels across a matrix of three fibroblast isolates and the three senescence inducers showed that PML-induced senescence leads to the smallest global changes with respect to decreased gene expression levels (-1.5-fold; $P<0.05$) when compared with proliferating cells, with 784 genes being affected, whereas Ras^{V12} and RS negatively affected 1989 ($\sim$2.5-fold more) and 3555 ($\sim$4.5-fold more) genes, respectively (Figure 1A). Previous studies have linked PML function to gene regulation, however, only a small number of genes have been shown to be directly downregulated by PML (Xu *et al*, 2004; Kumar *et al*, 2007). An one-to-one comparison of the PML senescence transcriptome either with the Ras^{V12} or with the RS transcriptomes indicated that it shared $\sim$62 and $\sim$50% of underexpressed genes, respectively. A set of 262 downregulated genes common to all three senescence transcriptomes was identified (Figure 1A; Supplementary Table S1). Among the genes being consistently underexpressed ($\sim$2–4-fold) in all

 ©2012 European Molecular Biology Organization

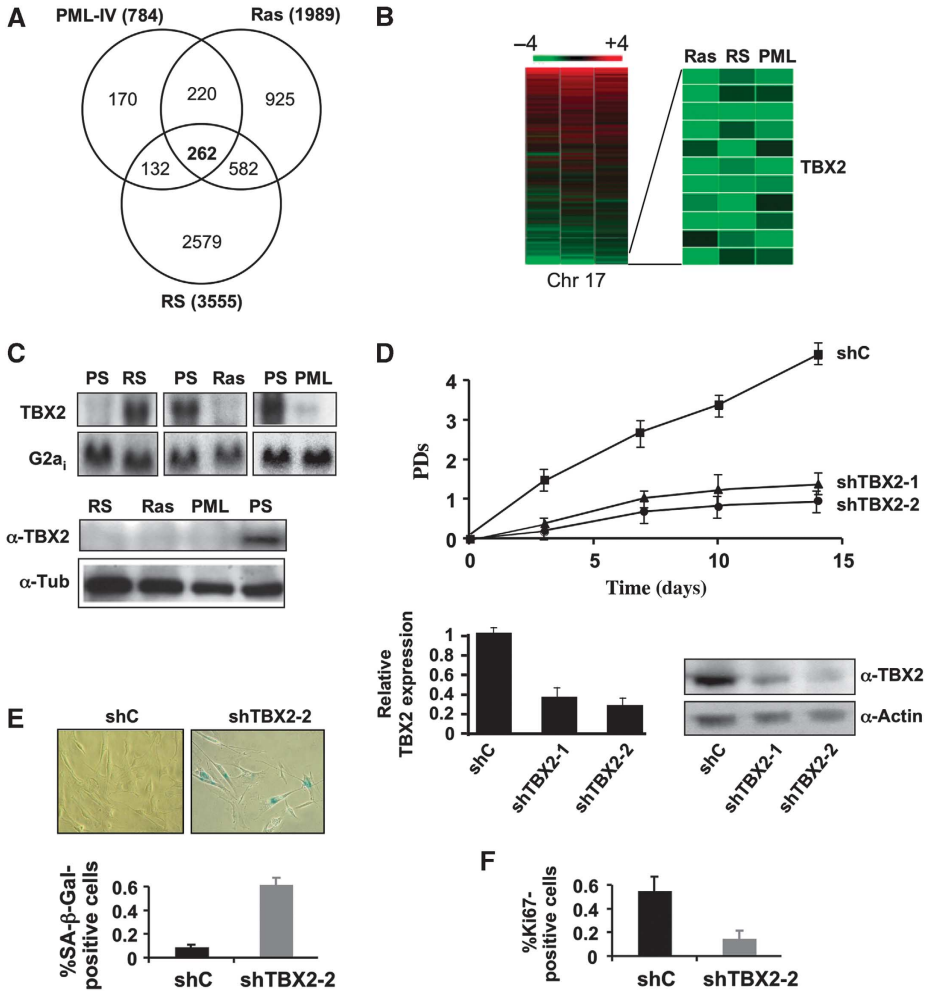

Figure 1 TBX2 repression actively contributes to onset of senescence. (**A**, **B**) *TBX2* gene expression is downregulated upon senescence in WI38 HDFs. (**A**) Venn diagram of common downregulated genes in WI38 fibroblasts undergoing PML-IV, Ras^{V12} or replicative senescence (RS) as compared with proliferating WI38 fibroblasts using Affymetrix transcriptome analysis. In brackets, total number of downregulated genes is given. (**B**) Representative heat map of underregulated genes on chromosome 17 to which TBX2 maps in the three senescent transcriptomes. (**C**) Relative quantification of TBX2 expression by northern (upper panel) and western blot analysis (lower panel) comparing WI38 fibroblasts undergoing PML-IV (IV), Ras^{V12} (Ras) or RS to pre-senescent WI38 fibroblasts (PS). *G2a$_i$* and Tubulin (Tub) serve as loading controls. (**D**–**F**) Depletion of TBX2 induces a senescence response in fibroblasts. (**D**) Proliferation curves of WI38 HDFs infected with pLKO.1-shScramble (shC), pLKO.1-shTBX2-1 or shTBX2-2 (shTBX2-1 and shTBX2-2). After drug selection, the number of population doublings (PDs) was determined over the indicated period of time. Day 0 is the first day after selection. PDs for each time point are the mean value of triplicates. Also, the expression of TBX2 using qRT–PCR (lower left panel) and western blot analysis (lower right panel) is shown. Actin served as loading control. (**E**) Percentage of infected WI38 HDFs staining positive for SA-β-Gal expression and (**F**) for proliferation marker Ki67 at day 10 post-selection. Plotted values: means ± s.e. of three independent counts of >200 cells.

senescent cells was TBX2 (Figure 1B). Because TBX2 has been shown to play a prominent role in oncogenesis (Abrahams *et al*, 2010), we decided to focus our further analysis on the function of this protein in senescence. To confirm the microarray results for TBX2 expression during senescence, we performed northern and western blot analysis (Figure 1C). Senescent cells induced either by replicative exhaustion (RS), Ras^{V12} or PML-IV displayed a pronounced reduction in both TBX2 transcript (upper panel) and protein levels (lower panel) when compared with pre-senescent cells or cells overexpressing PML isoforms PML-I or PML-III, the latter serving as proxies for other PML isoforms (Supplementary Figure S1B and C). Thus, the downregulation of TBX2 is coincident with the onset of senescence induced by different signals.

We then asked whether TBX2 repression on its own is sufficient to trigger a senescence response. To address this question, we stably silenced its expression by shRNA-mediated knockdown in WI38 fibroblasts using two individual knockdown constructs (shTBX2-1 and shTBX2-2). Remarkably, WI38 fibroblasts silenced for TBX2 expression displayed several features of senescent cells when compared with shControl (shC)-infected cells including a permanent proliferative arrest (Figure 1D), flat cell morphology and increase in cells positive for SA-β-Gal activity (Figure 1E) as well as a decrease in cells positive for Ki67 expression (Figure 1F). Together, these results argue that TBX2 repression is not merely associated with the senescence response but actively contributes to it.

TBX2 is a downstream target gene of PML

To explore the possibility that endogenous PML downregulates TBX2 expression *in vivo*, we first assessed TBX2 expression levels in PML$^{+/+}$ and PML$^{-/-}$ MEFs (Figure 2A).

©2012 European Molecular Biology Organization

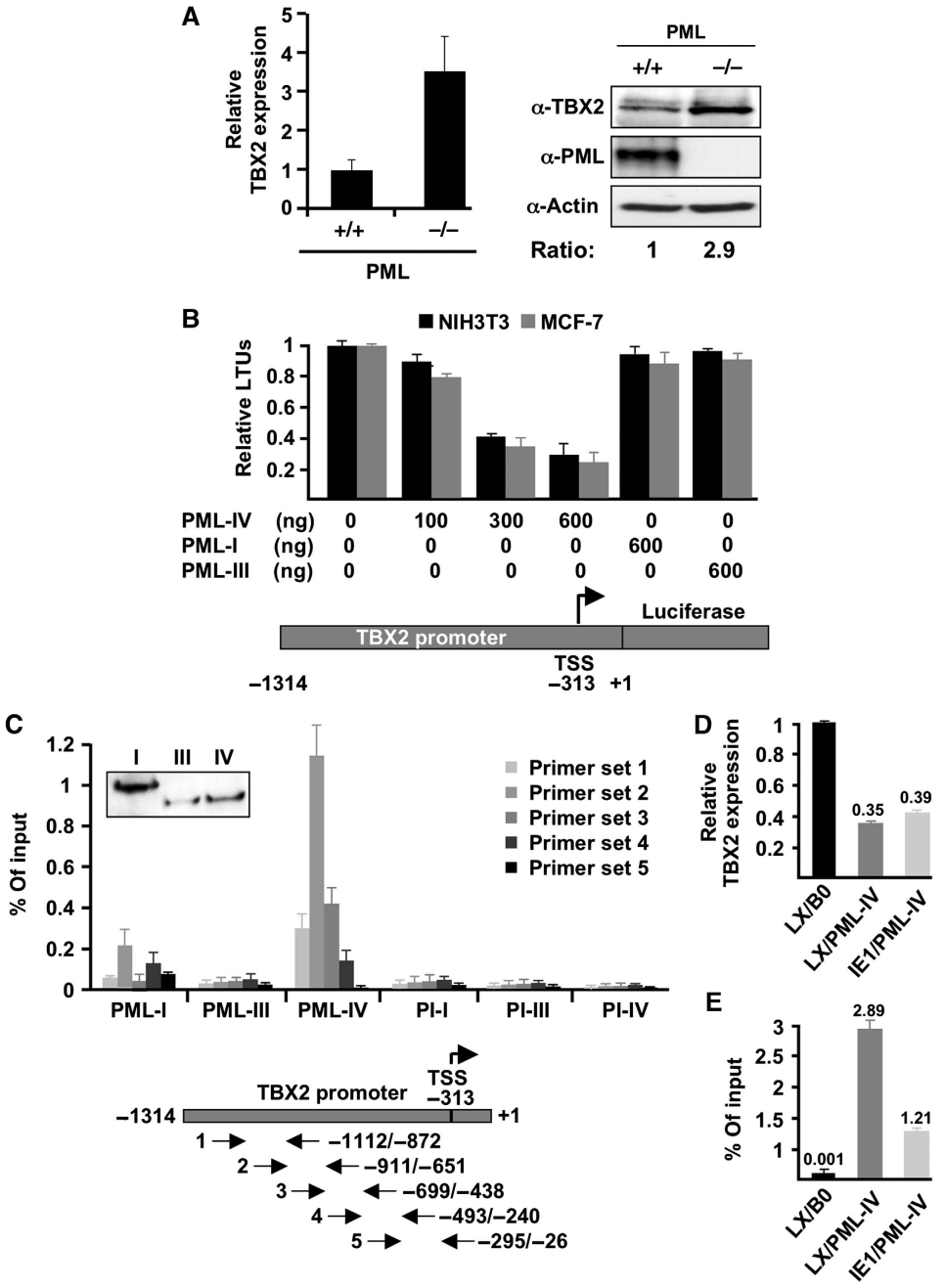

Figure 2 TBX2 is a downstream target gene of PML-IV in senescence. (**A**) *TBX2* gene expression is upregulated in $PML^{-/-}$ MEFs. Comparison of TBX2 transcript and protein level in $PML^{+/+}$ and $PML^{-/-}$ MEFs as measured by qRT–PCR (left panel) and western blot (right panel), respectively. GAPDH and actin served as internal normalization controls. (**B**) PML-IV represses *TBX2* gene expression in a dose-dependent manner. Promoter luciferase reporter assay conducted in NIH3T3 or MCF-7 cells co-transfected with the indicated amounts of PML-I, -III or -IV expression and TBX2 promoter luciferase-reporter vectors (comprising a 1314-bp *TBX2* promoter fragment from −1314 to +1 relative to the translational start site; TSS, putative TBX2 transcriptional start site). Plotted values are means ± s.e. of light transmission units (LTUs) of luciferase activity corrected for β-galactosidase activity for three independent experiments performed each in triplicates. (**C**) PML-IV is the predominant isoform to bind to the *TBX2* gene promoter. qChIP analysis of TBX2 promoter in PML-I, -III and -IV-overexpressing WI38 HDFs using anti-PML-I, -III and -IV antibodies or the corresponding pre-immune serum (PI) and primer sets 1–5 for qPCR. Cartoon for relative location of five PCR primer sets used for analysis of TBX2 promoter occupancy by PML is shown below. Inset depicts western blot of PML-I, III and -IV in respective overexpressing cells. (**D**) Relative *TBX2* gene expression as determined by qRT–PCR on total RNA prepared from WI38 HDFs expressing LX/B0, LX/PML-IV or IE1/PML-IV. (**E**) PML-IV qChIP analysis of *TBX2* gene promoter using primer set 2 (see Figure 2C) (lower panel) on chromatin prepared from same cells as in Figure 2D.

We detected a robust increase both in TBX2 transcript (~4-fold) and in protein levels (~3-fold) in $PML^{-/-}$ MEFs when compared with $PML^{+/+}$ MEFs as determined by qRT–PCR (left panel) and western blot analysis (right panel).

Next, we wanted to extend this finding to human cells and test PML transcriptional repressor activity in a reporter gene assay. We, therefore, cloned (from human genomic DNA) a ~1.3-kb promoter fragment from −1314 to +1 base pair

 ©2012 European Molecular Biology Organization

(bp) relative to the TBX2 translational start site into a luciferase-reporter plasmid. This promoter region has been described as being sufficient to direct TBX2 expression (Carreira *et al*, 2000; Teng *et al*, 2007). Co-transfection of this construct together with PML-IV or PML isoforms PML-I and PML-III in two different cell lines revealed a PML-IV-specific, dose-dependent reduction in promoter activity (Figure 2B) though expression of all PML isoforms was equal (data not shown). We then asked whether PML-IV could physically associate with the TBX2 promoter *in vivo* and whether this interaction might be PML-IV specific using quantitative ChIP (qChIP). WI38 fibroblasts retrovirally infected with PML-I, PML-III or PML-IV were prepared for ChIP 2 days post-selection and PML-I, PML-III or PML-IV/DNA complexes were pulled down either with in-house produced PML-I, PML-III or PML-IV polyclonal antibodies or with pre-immune serum (Supplementary Figure S2A–C). Precipitated DNA was subsequently analysed by qPCR using a set of five partially overlapping primer pairs spanning the 1.3-kb promoter region. We repeatedly detected a strong interaction of PML-IV with a TBX2 promoter sequence located between −911 and −651 bp (primer set 2) and weaker interactions with two adjacent promoter sequences situated between −1112/−872 and −699 and −438 bp (primer sets 1 and 3) upstream of the translation initiation codon. Conversely, the binding of PML-I or PML-III to these promoter sequences was significantly lower or undetectable (Figure 2C).

We previously showed that PML-induced senescence is independent from the integrity of PML NBs. We, therefore, asked whether or not TBX2 repression is equally independent from PML NBs using the cytomegaloviral protein IE1, which disrupts PML NBs without affecting the overall level of the various NB components (Bischof *et al*, 2002). Accordingly, we serially infected WI38 fibroblasts with empty, control vectors pLXSN (LX)/pBABE (B0), LX/PML-IV or IE1/PML-IV. Although PML NBs were completely disrupted in IE1/PML-IV-infected cells (Supplementary Figure S2D) neither induction of senescence was impeded, as previously reported (data not shown) (Bischof *et al*, 2005), nor *TBX2* gene repression (Figure 2D) while the association of PML-IV with the TBX2 promoter was diminished about 2.5-fold when compared with LX/PML-IV-expressing cells, but still about 1000-fold higher than in LX/B0 control cells (Figure 2E).

Altogether, these data show that PML-IV is the primary isoform to occupy the TBX2 promoter *in vivo* and to actively contribute to TBX2 transcriptional repression during senescence. Moreover, our data imply that the integrity of PML NBs is by-and-large dispensable for TBX2 repression but may aid in a more efficient recruitment of PML to the TBX2 promoter.

PML-IV interaction with the TBX2 promoter is dependent on a functional p130/E2F4 repressor complex

PML is devoid of any direct DNA binding capacity and therefore needs to piggyback transcription or chromatin interacting factors. Previous data by Vernier *et al* (2011) implicated PML in the regulation of Rb/E2F-response genes, and we therefore investigated whether or not TBX2 is an E2F-target gene. Interestingly, a recent genome-wide ChIP-seq analysis found that the Rb-family member p130 binds to the TBX2 promoter in senescent cells (Chicas *et al*, 2010). Based on this finding, we performed PML-IV, p130, Rb, E2F1 (predominantly interacts with Rb) and E2F4 (predominantly interacts with p130) qChIP analysis in cells overexpressing PML-IV. In parallel, we also conducted qChIP with an antibody directed against histone 3 dimethylated at lysine 9 ($H3K9_{me2}$), which marks inactive chromatin (Jenuwein, 2006). Indeed, as shown in Figure 3A, using PCR primer sets 1–5 spanning the TBX2 promoter region under investigation, we not only validated the predicted ChIP-seq association of p130 with the TBX2 promoter but more importantly, we also observed that the p130, E2F4 and $H3K9_{me2}$ qChIP peaks (i.e., primer sets 1–3) greatly overlapped with the one of PML-IV. By contrast, we did not detect any signal above background for Rb or E2F1 (data not shown). These data, thus, argue that a p130/E2F4 repressor complex may be important for the association of PML with the TBX2 promoter. To test this idea correct, we first performed endogenous co-immunoprecipitation experiments between PML and p130 or E2F4 in senescent WI38 fibroblasts. As depicted in Figure 3B, PML, p130 and E2F4 co-immunoprecipitated with each other, thus highlighting the physical interaction of these proteins under physiological conditions. Next, we used the viral oncoprotein HPV16E7 to disrupt the function of all Rb-family members, which should ablate the binding of PML-IV to the TBX2 promoter if indeed a p130/E2F4 complex was important for the binding of PML-IV to the promoter. We opted for E7 rather than shRNA-mediated knockdown of p130 because of a possible compensatory effect of the two other Rb proteins. As shown in Figure 3C, in LX/B0 and E7/PML-IV-expressing cells, we neither obtained a PML-IV nor p130 qChIP signal above background. By contrast, in LX/PML-IV and E7Δ21–24 (an Rb binding-deficient E7 mutant)/PML-IV-expressing cells, both PML-IV and p130 were present at the TBX2 promoter although the binding rate of PML-IV was diminished about 3-fold in E7Δ21–24/PML-IV compared with LX/PML-IV-expressing cells but was still about 1000-fold higher than in E7/PML-IV-expressing cells. Concordantly, we found that TBX2 expression was only repressed in LX/PML-IV and E7Δ21–24/PML-IV but not in LX/B0 and E7/PML-IV-expressing cells (Figure 3D). Combined these results indicate that TBX2 is a PML-repressible E2F-response gene and that association of PML-IV with the TBX2 promoter is dependent on a functional p130/E2F4 repressor complex, which is consistent with recent findings that the ability of E7 to rescue PML-induced senescence relies on its ability to negatively interfere with Rb/E2F function (Mallette *et al*, 2004; Bischof *et al*, 2005; Vernier *et al*, 2011).

TBX2 circumvents PML-IV-induced senescence

Overexpression of TBX2 has been shown to delay replicative senescence (Jacobs *et al*, 2000). Therefore, we sought to determine whether TBX2 could impact on PML-IV-induced senescence. To address this issue, we transduced WI38 fibroblasts first with the retroviral vector pDON (DON) or its derivative encoding TBX2, followed by superinfection either with pBABE expressing PML-IV or with empty vector (B0). Subsequently, we started monitoring the proliferative properties of infected cell populations by proliferation curves (population doubling, PD = 0; day = 0) and Ki67 immunostaining and evaluated the percentage of SA-β-Gal-positive cells (Figure 4A and B). Cells constitutively expressing DON/PML-IV rapidly entered senescence as previously reported (Bischof *et al*, 2002). In contrast, cells expressing

©2012 European Molecular Biology Organization

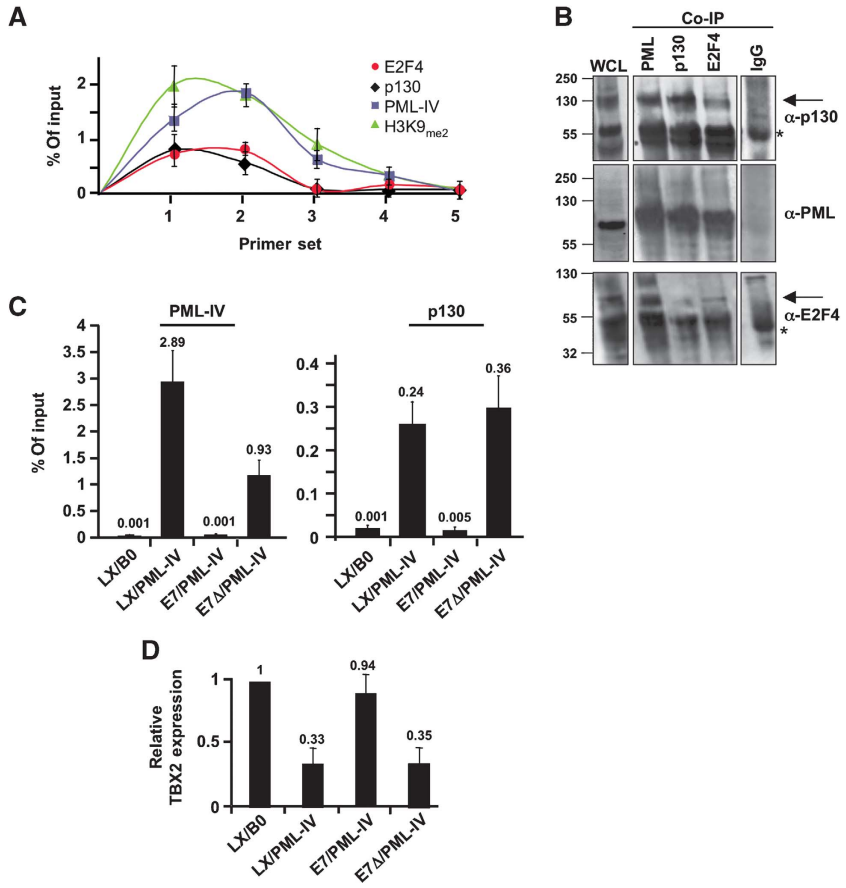

Figure 3 Association of PML-IV with TBX2 promoter depends on a functional p130/E2F4 repressor and is specific for senescence. (**A**) PML-IV, p130, E2F4 and H3K9$_{me2}$ qChIP analysis of *TBX2* gene promoter using primer sets 1–5 (see Figure 2C) on chromatin prepared from WI38 HDFs overexpressing PML-IV. All specific qChIP signals were corrected by substracting non-specific IgG qChIP signal. (**B**) Co-immunoprecipitation (Co-IP) of endogenous PML with p130 or E2F4 in replicative senescent WI38 HDFs using anti-PML antibody mix detecting PML isoforms I–V, p130, E2F4 or IgG. Western blot with anti-pan-PML, anti-p130 and anti-E2F4. WCL, whole-cell lysate. Asterisks, IgG heavy chain; arrows indicate p130 and E2F4 signals. (**C**) PML-IV and p130 qChIP analysis of *TBX2* gene promoter using primer set 2 (see Figure 2C) on chromatin prepared from WI38 HDFs ectopically expressing LX/B0, LX/PML-IV, E7/PML-IV or E7Δ21−24(E7Δ)/PML-IV. Specific qChIP signals were corrected by substracting non-specific IgG qChIP signal. (**D**) Relative TBX2 expression as determined by qRT–PCR on total RNA prepared from cells used in Figure 3C.

TBX2 in combination with PML-IV proliferated in a manner that was indistinguishable from TBX2/B0 control cells and both cell populations had an extended lifespan of ~6–8 PDs when compared with DON/B0 controls (Figure 4A). Additionally, TBX2/PML-IV-expressing cells stained positive for Ki67 and negative for SA-β-Gal when compared with DON/PML-IV cells (Figure 4B).

To identify the TBX2 domains required for abrogation of the PML-IV-dependent senescence response, we infected WI38 fibroblasts sequentially with control (DON) or either of two well-characterized TBX2 mutant retroviruses (TBX2ΔRD1; TBX2TB) and PML-IV or control retroviruses (B0). TBX2ΔRD1 lacks a recently identified repression domain (RD1) comprising amino acids (aa) 501–618, while TBX2TB harbours two consecutive point mutations in its DNA-binding TB domain (R122E and R123E), thus rendering this domain dysfunctional (Figure 4C). Both mutant proteins were shown to have an impaired capacity to rescue murine cells from senescence (Lingbeek *et al*, 2002). Cells co-expressing TBX2TB/PML-IV grew unimpeded similar to cells expressing TBX2/PML-IV. By contrast, cells expressing TBX2ΔRD1/PML-IV senesced as quickly as cells expressing PML-IV alone (Figure 4D). Each TBX2 mutant was expressed at levels similar to that of wild-type TBX2 and PML expression was also equal in all samples (Figure 4D). Therefore, the differential effect of each TBX2 mutant on PML-induced senescence is most likely explained by their ability to differentially interact with effector proteins and/or DNA-binding elements. Of note, TBX2 overexpression did not cause any visible alteration in PML NB architecture (Supplementary Figure S3A) and, in line with this finding, we did not detect any TBX2 in PML NBs (data not shown).

TBX2 and TBX3 are closely related paralogues and both proteins share a high degree of sequence conservation in their DNA-binding and repression domains. To assess the capacity of TBX3 to inhibit PML-IV-induced senescence, we infected WI38 fibroblasts sequentially with DON or TBX3 retroviruses and PML-IV or B0. Consistent with the close homology between TBX2 and TBX3, the latter was able to inhibit senescence elicited by PML-IV (Supplementary Figure S3B). Together, these results demonstrate that TBX2 and its paralogue TBX3 are potent inhibitors of PML-IV-mediated senescence and that this inhibitory effect is linked to the C-terminal repression domain RD1.

 ©2012 European Molecular Biology Organization

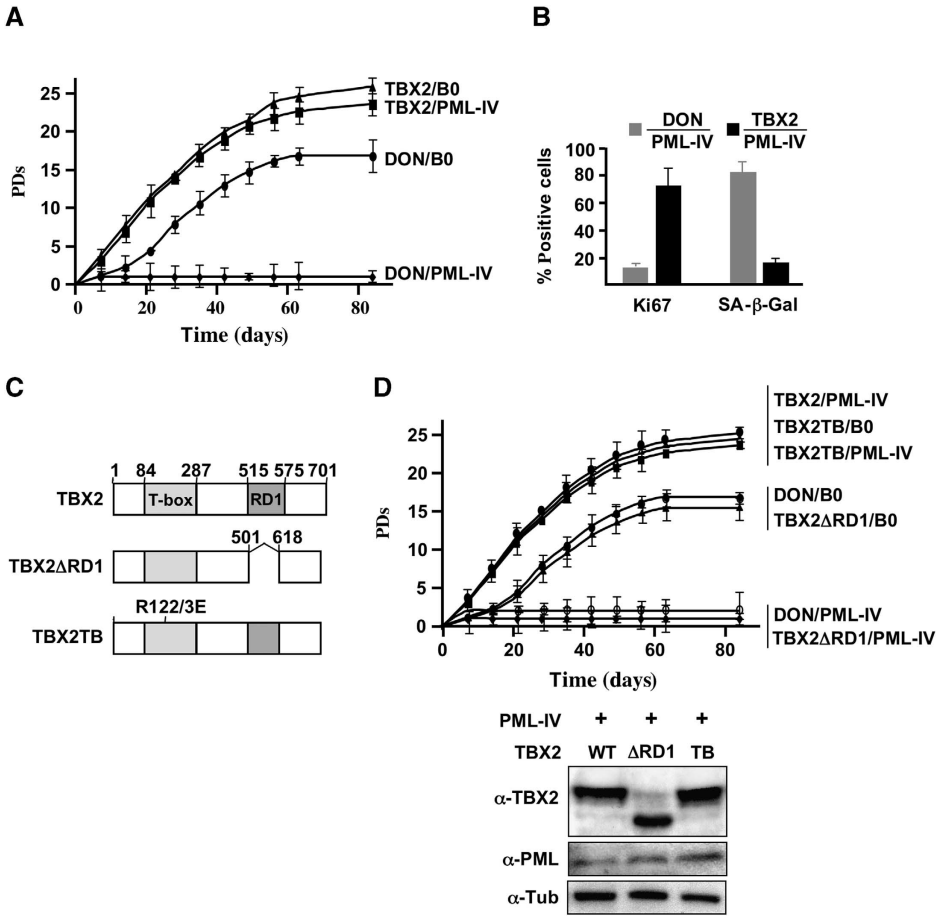

Figure 4 Inhibition of PML-IV-induced senescence by TBX2 depends on its repression domain. (**A**, **B**) TBX2 overexpression bypasses PML-IV-induced senescence. (**A**) Proliferation curves of WI38 HDFs expressing combinations of TBX2 or empty vector (DON) plus PML-IV or empty vector (B0). After drug selection, the number of population doublings (PD) was determined over the indicated time period. Day 0 is the first day after selection. PDs for each time point are the mean value of triplicates. (**B**) Percentage of DON/PML-IV- and TBX2/PML-IV-infected WI38 HDFs staining positive for proliferation marker Ki67 and SA-β-Gal at day 10 post-selection. Plotted values: means ± s.e. of three independent counts of >200 cells. (**C**, **D**) C-terminal repression domain RD1 of TBX2 is essential for abrogation of senescence elicited by PML-IV. (**C**) Schematic representation of TBX2 domains and mutants used in this study: repression domain 1 (RD1), T-box DNA-binding domain (TB). TBX2ΔRD1, deleted for amino acids (aa) 501–618; TBX2TB, R122E, R123E aa replacements in T-box. (**D**) Proliferation curves of WI38 HDFs superinfected with retroviruses expressing combinations of TBX2, TBX2ΔRD1 or TBX2TB or empty vector (DON) plus PML-IV or empty vector (B0). After drug selection, the number of PDs was determined over the indicated period of time. Day 0 is the first day after selection. PDs for each time point are the mean value of triplicates. Relative quantification of protein levels of TBX2 constructs and PML-IV by western blot is also shown below.

TBX2 interacts with PML and inhibits its transcriptional repressor function

The RD1 domain of TBX2 was proposed to function as a protein–protein interaction module involved in recruiting other proteins (Lingbeek *et al*, 2002; Vance *et al*, 2005). Therefore, we tested the possibility that TBX2 might target PML directly. Accordingly, we performed co-immunoprecipitation experiments in U2OS cells co-transfected with vectors expressing FLAG–PML-IV and either TBX2 or TBX2ΔRD1, or appropriate empty vectors. As shown in Figure 5A, FLAG–PML-IV co-immunoprecipitated with wild-type TBX2, while the ΔRD1 mutant had a largely diminished ability to interact with PML (compare lanes 5 and 6), thus demonstrating that PML-IV interacts with TBX2 *in vivo* and that the RD1 domain of TBX2 is instrumental for this interaction to occur efficiently. Of note, binding of TBX2 was not exclusive for PML-IV but extended to other PML isoforms (Supplementary Figure S4A). Moreover, the TBX2 paralogue TBX3 also strongly interacted with PML-IV (Supplementary Figure S4B). To enhance the physiological relevance for the observed interaction, we carried out endogenous co-immunoprecipitation experiments between PML and TBX2 in low passage, proliferating WI38 fibroblasts. As depicted in Figure 5B, both proteins could be co-immunoprecipitated in reciprocal pull-down experiments, thus highlighting the physical association of the two proteins under physiological conditions.

Given the physical interaction between TBX2 and PML in proliferating cells, we then assessed the capacity of TBX2 to prevent PML-mediated repression of *TBX2* gene expression *in vivo*. To this end, we first determined the relative promoter activity of the TBX2 promoter by co-transfecting NIH3T3 murine fibroblasts with the TBX2 promoter-reporter construct together with a stable amount of PML-IV along with increasing amounts of TBX2 or a fixed amount of TBX2ΔRD1 and a normalization control. As shown in Figure 5C, TBX2,

©2012 European Molecular Biology Organization

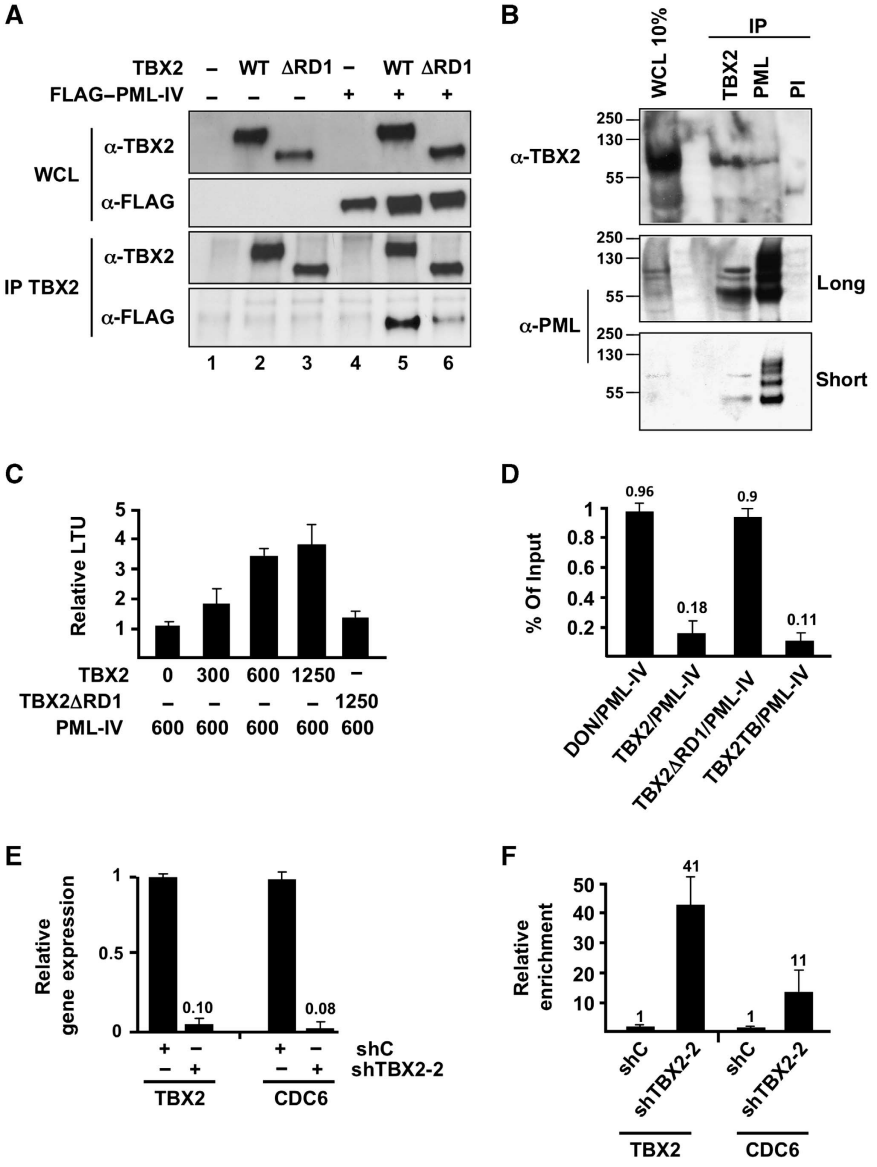

Figure 5 TBX2 associates with PML-IV and negatively interferes with PML-IV function. (**A**, **B**) PML-IV and TBX2 interact *in vivo* and RD1 of TBX2 is required for interaction. (**A**) Immunoprecipitation (IP) with anti-TBX2 antibody in cellular lysates prepared from U2OS cells expressing combinations of FLAG–PML-IV or empty vector and TBX2 or TBX2ΔRD1. Immunocomplexes were analysed by western blot with antibodies specific for FLAG and TBX2. WCL, whole-cell lysate, 2.5% of total used for IP. (**B**) Co-immunoprecipitation (Co-IP) of endogenous PML with TBX2 in pre-senescent, proliferating WI38 HDFs, using anti-PML antibody mix detecting PML isoforms I–V, anti-TBX2 or pre-immune serum (PI). Western blot with anti-pan-PML and anti-TBX2. WCL, whole-cell lysate. (**C**, **D**) TBX2 perturbs PML-IV transcriptional repressor function. (**C**) Luciferase-reporter assay in NIH3T3 cells co-transfected with the indicated amounts (ng) of FLAG–PML-IV and TBX2 (wild-type or RD1 mutant) expression vectors, TBX2 luciferase-promoter reporter and pCMV-β-galactosidase vector for normalization. Plotted values: means ± s.e. of light transmission units (LTUs) of luciferase activity corrected for β-galactosidase activity for three independent experiments performed in triplicates. (**D**) PML-IV qChIP analysis of *TBX2* gene promoter in WI38 HDFs infected with DON/PML-IV, TBX2/PML-IV, TBX2ΔRD1/PML-IV or TBX2TB/PML-IV using qPCR primer set 2 (see Figure 2C). (**E**) Relative gene expression of TBX2 and CDC6 as determined by qRT–PCR on total RNA prepared from cells infected either with pLKO.1-sh-Control (shC) or pLKO.1-shTBX2-2 (shTBX2-2). (**F**) PML-IV qChIP analysis of *TBX2* and *CDC6* gene promoters in cells from Figure 5E. PML-IV qChIP signals were corrected by substracting non-specific pre-immune serum qChIP signal.

but not TBX2ΔRD1, was able to derepress PML-mediated repression of the TBX2 promoter in a dose-dependent manner though expression of both TBX2 constructs was equal (data not shown). This result led us to evaluate whether TBX2 is able to diminish physical presence of PML at the TBX2 promoter *in vivo* using PML-IV qChIP in WI38 fibroblasts stably expressing DON/PML-IV, TBX2/PML-IV, TBX2ΔRD1/PML-IV or TBX2TB/PML-IV. In cells overexpressing TBX2/PML-IV or TBX2TB/PML-IV, the amount of PML bound to the TBX2 promoter DNA was reduced ~6–10-fold when compared with cells overexpressing PML-IV alone or in conjunction with TBX2ΔRD1 (Figure 5D; Supplementary Figure S5A and B). Together with the above results, these data strongly imply that TBX2 inhibits PML transcriptional repressor function through direct protein–protein interaction *via* its C-terminal RD1 domain. To further corroborate this notion,

 ©2012 European Molecular Biology Organization

we rendered cells senescent by stably expressing TBX2 targeting shRNA (see Figure 1D–F), which should liberate senescence-associated PML transcriptional repressor activity from the inhibitory effect of TBX2. To monitor an increase in this activity, we combined qRT–PCR and PML-IV qChIP to analyse the *TBX2* gene and PML-repressible E2F-target genes CDC6, BUB1, ORC6L, USP1, ASF1B, BRCA1, NEK2, CDC2 and CCNA2 (Vernier *et al*, 2011). As depicted in Figure 5E and Supplementary Figure S5C, we observed a robust decrease in transcript abundance for TBX2, CDC6 (Figure 5E), ORC6L, USP1, ASF1B, BRCA1, NEK2, CDC2, CCNA2 and BUB1 (Supplementary Figure S5C) in shTBX2-2 but not shControl (shC)-expressing cells and this effect was readily reversed in E7/PML-IV-expressing cells (data not shown). Strikingly, PML-IV was strongly enriched at the TBX2 (~40-fold) and CDC6 (~10-fold) promoters in shTBX2-2 when compared with shC-expressing cells (Figure 5F). The CDC6 promoter binding site of PML-IV is located between 604 and 432 bp upstream of the translation initiation codon, and thus falls into a region that was previously identified as an Rb/p130 binding region in senescent cells by ChIP-seq (Chicas *et al*, 2010). Combined these data imply that the physical release of PML from TBX2 enhances PML pro-senescence activity as evidenced by an increased PML binding to and repression of its target genes.

Endogenous PML mediates TBX2 repression upon senescence but not quiescence

Our results indicated that TBX2 expression is tightly linked to cell proliferation and that, conversely, its repression is associated with senescence. Moreover, we observed that PML is a potent repressor of TBX2 expression and that, in turn, TBX2 is able to inhibit PML function through direct interaction. Overexpression of Ras^{V12} produces an initial mitogenic stimulus followed by the onset of cellular senescence both in human fibroblasts and in MEFs (Serrano *et al*, 1997; Lin *et al*, 1998). Therefore, this experimental model is ideal to probe the existence of a positive correlation between the relative expression levels of TBX2 and PML and the presence of PML at the TBX2 promoter combining expression profiling by qRT–PCR with qChIP at different time points in WI38 fibroblasts undergoing Ras^{V12} senescence.

To further facilitate this analysis, we transduced WI38 fibroblasts with a retrovirus expressing a conditional Ras^{V12} oncoprotein, obtained by fusing downstream of a tamoxifen (4OHT)-sensitive mutant of the oestrogen receptor ligand binding domain (ER^{Tam}:Ras^{V12}) (Tarutani *et al*, 2003). Cells expressing 4OHT-activated Ras^{V12} initially proliferated before they underwent senescence as evidenced by their proliferative arrest and increase in the percentage of SA-β-Gal-positive cells (Figure 6A), while control-treated Ras^{V12} cells proliferated unimpeded (data not shown). We prepared total RNA from these cells at different time points (days 0–7) for qRT–PCR analysis and performed qChIP analysis using antibodies directed against PML-I, PML-III, PML-IV, histone 3 trimethylated at lysine 27 ($H3K27_{me3}$) and histone 3 trimethylated at lysine 4 ($H3K4_{me3}$). Transcriptionally repressed regions of chromatin are marked by $H3K27_{me3}$, whereas $H3K4_{me3}$ marks transcriptionally active chromatin (Jenuwein, 2006). These two histone modifications were chosen to track and correlate the activation status of the TBX2 promoter with the presence of PML at this promoter. As seen in Figure 6B, expression profiling of TBX2 and PML over the above indicated time period revealed a peak in TBX2 transcript abundance between days 1 and 2 post-4OHT-treatment (i.e., a time where cells underwent Ras^{V12}-driven proliferation and had relatively low SA-β-Gal activity; see Figure 6A). Thereafter, TBX2 expression dropped significantly over the next 5 days to reach its lowest point at day 7 post-induction when the cell population was fully senescent. By contrast, PML expression incrementally increased from days 2 to 7. Simultaneous qChIP analysis of the TBX2 promoter with anti-PML-I, PML-III, PML-IV, PML-$H3K27_{me3}$ and PML-$H3K4_{me3}$ antibodies over the same time period revealed that, at the time point where TBX2 transcript levels were high, the transcriptionally active chromatin mark $H3K4_{me3}$ was also enriched at the TBX2 promoter whereas physical presence of PML-IV was relatively low. Conversely, at the later time points at which TBX2 expression had dropped, physical presence of PML-IV as well as the repressive chromatin mark $H3K27_{me3}$ was increased at the TBX2 promoter, whereas PML-I and PML-III and the active chromatin mark $H3K4_{me3}$ were barely detectable (Figure 6C; Supplementary Figure S6A and B). These data reinforce the notion that PML-IV is the predominant PML isoform to control senescence-associated TBX2 repression.

The above findings positively correlated PML-IV presence at the TBX2 promoter with TBX2 repression in Ras^{V12}-induced senescent cells, strongly suggesting that PML-IV could actively contribute to this inhibition. To further corroborate this result, we determined TBX2 expression levels in Ras^{V12}-expressing $PML^{+/+}$ and $PML^{-/-}$ MEFs at different time points. As shown in Figure 6D, we detected a transient increase in TBX2 expression in $PML^{+/+}$ MEFs at day 4 post-selection after which its expression declined coincidental with the onset of senescence. By contrast, increased TBX2 expression levels persisted in $PML^{-/-}$ MEFs beyond day 4 and stayed constantly high until day 7. This result is consistent with the known resistance of $PML^{-/-}$ MEFs to engage Ras^{V12}-driven senescence (Pearson *et al*, 2000; de Stanchina *et al*, 2004) and the propensity of increased levels of TBX2 to facilitate senescence bypass (Jacobs *et al*, 2000).

We then asked whether PML-mediated TBX2 repression is specific for senescence or also occurs in quiescence. Accordingly, we compared TBX2 expression as well as PML-IV presence at the TBX2 promoter between pre-senescent (PS), quiescent (Q) and RAS senescent (S) cells using qRT–PCR, immunoblot and qChIP analysis. Although we observed reduced TBX2 transcript and protein levels in both quiescent and senescent cells when compared with pre-senescent cells (Figure 6E), we could, however, only barely detect PML-IV at the TBX2 promoter in quiescent cells, whereas PML-IV was readily detectable at the promoter in senescent cells (Figure 6F). These results, thus, indicate that PML-dependent repression of TBX2 is tightly linked to the essentially irreversible cell-cycle arrest of senescence and does not play a major role in the reversible cell-cycle arrest of quiescence.

In conclusion, the above data emphasize the requirement for PML, and in particular PML-IV, in TBX2 repression during senescence but not quiescence. Moreover, these results allude to the existence of threshold-specific requirements for the functional inhibition of PML by TBX2 and, conversely, the PML-directed transcriptional repression of TBX2 (Figure 7).

©2012 European Molecular Biology Organization

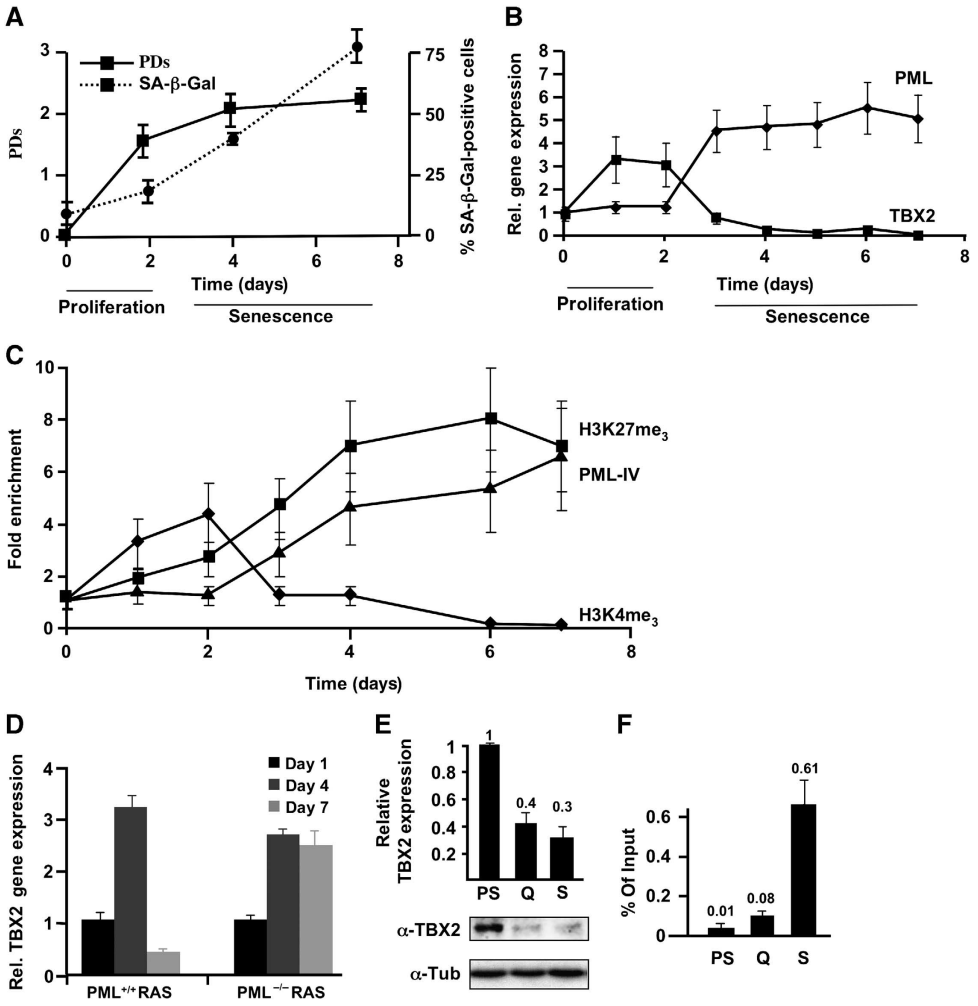

Figure 6 PML actively contributes to *TBX2* gene repression in Ras^{V12}-induced senescence but not quiescence. (**A**) Proliferation curve (solid line) and percentage of cells staining positive for SA-β-Gal (dashed line) of WI38 HDFs undergoing ER:Ras^{V12}-induced senescence. (**B**) Relative gene expression of PML and TBX2 as measured by qRT–PCR at the indicated time points on total RNA prepared from EtOH- and 4OHT-treated ER:Ras^{V12} WI38 HDFs. Plotted is the relative difference between EtOH- and 4OHT-treated cells. (**C**) TBX2 repression coincides with increased PML presence and repressive chromatin state at TBX2 promoter. Anti-PML-IV, -H3K27$_{me3}$ and -H3K4$_{me3}$ qChIP analysis of the *TBX2* gene promoter using primer set 2 (see Figure 2C) in EtOH- versus 4OHT-treated ER:Ras^{V12} cells. Relative fold enrichment at the indicated time points between EtOH- versus 4OHT-treated ER:Ras^{V12} cells is shown. (**D**) Comparison of TBX2 transcript abundance as determined by qRT–PCR at days 1, 4 and 7 post-selection in PML$^{+/+}$ and PML$^{-/-}$ MEFs undergoing Ras^{V12}-induced senescence. (**E**) Relative TBX2 expression as determined by qRT–PCR (upper panel) and western blot (lower panel) in pre-senescent (PS), quiescent (Q) and Ras^{V12}-senescent (S) WI38 HDFs. (**F**) PML-IV qChIP analysis of *TBX2* gene promoter using primer set 2 (see Figure 2C) on chromatin prepared from pre-senescent (PS), quiescent (Q) and Ras^{V12}-senescent (S) WI38 HDFs.

Discussion

In the present study, we identify the putative proto-oncogene TBX2 both as a negative regulator of PML function in the establishment of the senescence phenotype and as a novel senescence-specific PML-IV-repressible E2F-target gene. Recruitment of PML-IV to the TBX2 promoter and the ensuing PML-mediated transcriptional gene repression of TBX2 are dependent on a functional p130/E2F4 repressor complex but independent from the integrity of PML NBs. The functional relationship between TBX2 and PML is dictated by their respective protein levels. While elevated TBX2 levels inhibit PML-IV pro-senescence function through direct protein–protein interaction, increased PML levels actively contribute to TBX2 transcriptional repression in cells undergoing senescence but not quiescence. Thus, the activation statuses of TBX2 and PML precisely mirror the kinetics of the senescence process in mammalian cells (Figure 7). Consistently, PML-deficient cells have constitutively elevated TBX2 levels reflecting their known resistance to undergo senescence. Together, our results provide evidence for an autoregulatory loop linking PML and TBX2 function in senescence induction.

Role of PML in senescence-associated gene regulation

Senescence is a genetically driven process, therefore, the senescent phenotype induced by replicative exhaustion, Ras^{V12}, PML-IV and other stimuli is a function of gene expression changes. PML and by inference PML NBs have long been considered as factors involved in regulation of gene expression (Zhong *et al*, 2000). Direct evidence for this involvement is, however, scarce and to date, only a few direct PML gene targets have been identified and

 ©2012 European Molecular Biology Organization

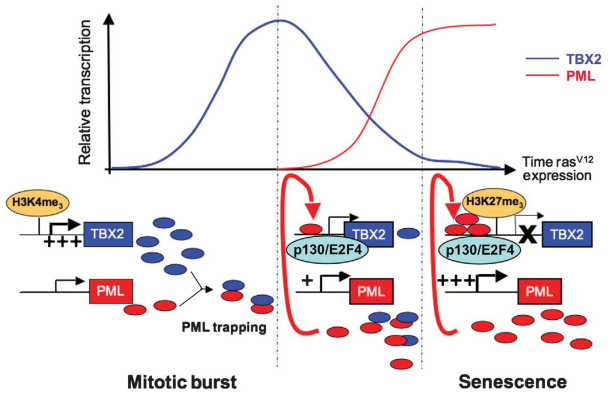

Figure 7 Model for PML/TBX2 functional interaction during senescence. PML and TBX2 activities are governed by their respective intracellular protein levels. Under (hyper)mitogenic conditions, such as after overexpression of oncogenic Ras^{V12} in primary fibroblasts, TBX2 is highly expressed (blue curve). The latter is reflected by an active chromatin state at the TBX2 promoter represented by the presence of H3K4$_{me3}$. The elevated TBX2 protein level squelches PML pro-senescence function(s) through direct protein–protein interaction. As cells enter senescence, PML expression increases progressively (red curve) and it is gradually recruited to the TBX2 promoter to implement an inactive chromatin state (marked by H3K27$_{me3}$ and H3K9$_{me2}$ (not shown)) in conjunction with a p130/E2F4 repressor complex, which ultimately shut-down *TBX2* gene expression in an essentially irreversible fashion.

studied precisely. Moreover, the exact mechanism as to how PML regulates changes in gene expression remains largely unexplored. In this regard, we recently provided the first evidence that individual PML isoforms can specifically impact on chromatin architecture and transcriptional output of certain genomic loci (Kumar *et al*, 2007). To get more insight into the transcriptional activities of PML, we employed gene expression profiling of senescent cells as an entry point to identify senescence-associated PML-target genes and we decided to concentrate our efforts on downregulated genes, a number of which have been shown to be important for the senescence process (Jacobs *et al*, 1999; Courtois-Cox *et al*, 2006; Gabai *et al*, 2009). Comparison of the PML-IV, Ras^{V12} and replicative senescence transcriptomes identified a set of 262 underexpressed genes that is common between them and thus signifies a core set of repressed genes in senescence. Given that PML-IV is a downstream effector in senescence induced by oncogenic Ras^{V12} and replicative exhaustion (Ferbeyre *et al*, 2000; Pearson *et al*, 2000; Bischof *et al*, 2002), the core set of repressed genes represented potential PML-repressible target genes. The anti-senescence factor and transcriptional repressor TBX2 was among this core set of genes that was consistently underexpressed in all senescent cells. We convincingly determined that PML-IV actively contributes to TBX2 repression in senescence. First, overexpression of PML-IV significantly reduced the expression of TBX2. Second, co-transfection experiments demonstrated that PML-IV represses transactivation of the *TBX2* promoter. Third, PML-IV is the major isoform to physically interact with the TBX2 promoter and its promoter presence coincides with the appearance of the transcriptionally inactive chromatin marks of H3K9$_{me2}$ and H3K27$_{me3}$ in senescence. Finally, PML-deficient cells express constantly high levels of TBX2 even after a senescence stimulus.

How might PML mediate TBX2 repression? PML is devoid of any DNA-binding activity, and therefore it is mandatory for it to associate with other DNA-binding protein(s) to regulate transcription. The promoter region that is targeted by PML contains p130 binding sites that were previously identified in a ChIP-seq analysis conducted on chromatin prepared from senescent cells (Chicas *et al*, 2010). The transcriptional repressor E2F4 represses transcription especially in quiescent cells through the recruitment of p130 to target promoters (Takahashi *et al*, 2000; Cam *et al*, 2004). Based on this data, we probed the possibility that TBX2 is an E2F-target gene and that a p130/E2F4 repressor complex is involved in the transcriptional regulation of the *TBX2* gene in senescence. Indeed, we demonstrated that p130 as well as E2F4 associated with the TBX2 promoter in senescent cells, and that their promoter binding region strongly overlapped with the one of PML-IV. By contrast, Rb and E2F1, which have been postulated to play the major role in the repression of E2F targets in senescence (Narita *et al*, 2003), were beyond detectability indicating that p130 repressor complexes may play an important role in senescence-associated repression of E2F-target genes. In line with the crucial role for the p130/E2F4 repressor complex in tethering of PML-IV to the TBX2 promoter, we found that p130 and E2F4 physically interact with PML in senescent cells and that disrupting p130/E2F4 function with the viral oncoprotein HPV16E7 ablated binding of PML-IV to the TBX2 promoter, activated TBX2 expression and bypassed PML-induced senescence. Perturbation of p130 and PML association with the TBX2 promoter was tightly linked to E7's ability to bind to p130 as a p130 binding-deficient E7 mutant protein E7Δ21–24 was no longer able to inhibit PML-induced TBX2 repression. Of note, E7Δ21–24 expression diminished the PML binding rate to the TBX2 promoter ~3-fold in senescent cells and this may be linked to its inherent ability to bind to PML as strong as wild-type E7 (Bischof *et al*, 2005). Since it did not, however, effectively reverse PML-induced TBX2 repression, we believe, therefore, that this mutant may have distinct PML binding properties, which still permit formation and functioning of the PML–p130 repressor complex. A similar mechanism has been proposed for the PML–p53–CBP transcriptional activator complex, which still binds to the mutant protein E7Δ21–24, yet its enzymatic activity is not affected by this binding (Bischof *et al*, 2005).

The nuclear function of PML NBs is still enigmatic. Our previous data indicated that senescence elicited by PML-IV is independent from the integrity of PML NBs by disrupting the latter with the cytomegaloviral protein IE1 (Bischof *et al*, 2002). In this communication, we now show that TBX2 repression is equally independent from PML NBs although the binding of PML-IV to the TBX2 promoter is reduced by ~2.5-fold in IE1/PML-IV co-expressing cells. This result thus seems to argue that PML NBs may be important for the most efficient targeting of PML response genes and that functional PML NBs may create a 'microenvironment' that is particularly competent for transcriptional regulation (Block *et al*, 2006). Congruent with this notion E2F-transcription factors and Rb colocalize with PML NBs in senescent cells though the functional relevance for this colocalization needs to be determined (Vernier *et al*, 2011).

Interestingly, PML is uniquely required for TBX2 repression in senescence but not quiescence. E2F4/p130 repressor

©2012 European Molecular Biology Organization

complexes are known to be most active in quiescent cells and we do find p130 also bound to the TBX2 promoter in quiescent cells (our unpublished data). We, therefore, champion the idea that PML presence at the TBX2 promoter tilts the balance from a reversible inactive chromatin state that exists in quiescence towards an essentially arrested inactive chromatin state that exists in senescence and that this state is marked by a combination of stable repressive chromatin marks including $H3K9_{me2}$ and $H3K27_{me3}$. This idea is supported by the known affinity of PML to physically associate with a variety of transcriptional corepressors including histonemethylases (HMTs) enhancer of zest 2 (EZH2), Suv39H1 (Villa *et al*, 2007), the NCoR/SMRT complex and histone deacetylases HDAC-1 and HDAC-3 (Minucci *et al*, 2001).

TBX2 and TBX3: potent inhibitors of the pro-senescence function of PML

A major finding of this study is the demonstration that TBX2 and its paralogue TBX3 are potent negative regulators of PML function in cellular senescence. Prior to this work, the best-characterized negative regulators of PML function were PML-RARα (Mann *et al*, 2001) and viral (onco)proteins (Everett and Chelbi-Alix, 2007). Our demonstration that TBX2 directly targets PML thus provides additional insights into the regulation and role(s) of PML in senescence. TBX2/3 are members of the T-Box family of transcriptional regulators, with roles in embryonic development and oncogenesis (Abrahams *et al*, 2010). Both proteins share a high degree of primary sequence conservation in their TB DNA-binding domain (Agulnik *et al*, 1995). During mouse oncogenesis, TBX2 and TBX3 functions have been associated predominantly with repression of the tumour suppressor genes $p19^{ARF}$ ($p14^{ARF}$ in human) and the cyclin-dependent kinase (CDK) inhibitor $p21^{CIP}$, though there is evidence for the repression of other tumour suppressors including CDK inhibitors $p15^{INK4b}$ and $p16^{INK4a}$ (Jacobs *et al*, 2000; Prince *et al*, 2004). Decreased expression of $p16^{INK4a}$, $p19^{ARF}$ and $p21^{CIP}$ invariably blunt Rb and p53 tumour suppressor activities, thus setting the stage for senescence bypass, immortalization and eventual transformation of cells. This being said, it is, however, important to recognize that, to date, most conclusions linking TBX2/3 function to cancerogenesis have been obtained almost exclusively from functional studies performed in murine cell lines. Thus, the oncogenic potential of TBX2/3 in human cells remains poorly understood. Here, we add novel insights into TBX2 anti-senescence function in human cells. Our data strongly suggest that TBX2 inhibits PML-IV pro-senescence function mainly through direct protein–protein interaction. First, PML and TBX2 interact in proliferating cells. Second, excessive TBX2 levels prevent both PML-mediated TBX2 repression and PML presence at the TBX2 promoter after a senescence stimulus (see above paragraph) and finally, cells depleted of TBX2 exhibit an increased PML pro-senescence activity, as exemplified by the enhanced promoter binding of PML to the repressed TBX2 and E2F-target gene *CDC6*. The inhibitory effect of TBX2 on PML function is independent from its DNA-binding TB domain but dependent on the C-terminal repressor domain RD1. Accordingly, disruption of RD1 allows PML-induced senescence to occur while disabling the TB domain leaves the anti-senescence property of TBX2 intact. These data establish a dominant role for RD1 in the inhibition of PML pro-senescence function and identify RD1 as an essential module for protein–protein interactions. The latter observations are in agreement with a previous report stating that an interaction between TBX2 and HDAC1 depends on the presence of the C-terminal portion of TBX2 (Vance *et al*, 2005). Of note, binding of TBX2/3 is not restricted to PML-IV alone but is also found between TBX2 and other PML isoforms. Therefore, it is likely that other PML isoform-specific functions involved in cellular homeostasis are equally compromised. In aggregate, we unravel inhibition of PML function as an important mechanism by which TBX2 facilitates senescence bypass and immortalization. Moreover, the results presented here reinforce the functional importance of PML in the establishment of the senescence phenotype, and thus in tumour suppression.

A Ying and Yang relationship of TBX2 and PML in the control of tumourigenesis and senescence

PML (and in particular PML-IV) has been shown to be a pivotal player in the establishment of the senescence phenotype by regulating the p53 and Rb tumour suppressor pathways (Ferbeyre *et al*, 2000; Pearson *et al*, 2000; Bischof *et al*, 2002; de Stanchina *et al*, 2004). The tumour-suppressive function of PML is highlighted by the fact that PML knockout mice are more tumour prone (Wang *et al*, 1998) and that PML protein levels were found to be significantly reduced in cancers of different histologic origin (Gurrieri *et al*, 2004a, b). These data demonstrate that steady-state levels of PML may be instrumental for proliferative homeostasis. In contrast, excessive protein levels of TBX2 and TBX3 have been detected in primary human breast and pancreatic cancers and various cancer cell lines (Abrahams *et al*, 2010). Thus, there is an inverse correlation between TBX2 and PML protein expression in many different cancer types. Our analysis provides some clues as to the mechanism underlying high TBX2 expression levels in some of these cancerous lesions, which is graphically depicted in our working model in Figure 7. Using Ras^{V12}-driven senescence as our experimental model system, we show that during an initial hypermitogenic phase TBX2 levels are significantly increased. During this phase, elevated TBX2 levels (and possibly TBX3 levels) potentiate Ras^{V12}-stimulated entry into the cell cycle by blocking the action of anti-proliferative forces including PML, $p16^{INK4a}$, $p14^{ARF}$ and $p21^{CIP}$. This initial burst in proliferation is followed shortly after by a senescence arrest that is accompanied by increased PML expression. This increase expedites the implementation of a robust senescence response by activating p53/Rb tumour suppressor functions and blocking counter-productive pro-proliferative signals including repression of TBX2. By contrast, loss of PML function or insufficient PML levels, as observed in several cancers, may fail to keep TBX2 expression in check and, thus, help to provide an environment conducive for immortalization and eventual transformation. The latter notion is corroborated by our findings that in PML-deficient cells the levels of TBX2 are persistently high compared with wild-type cells and these cells are refractory to Ras^{V12}-induced senescence and more prone to immortalize (Ferbeyre *et al*, 2000; Pearson *et al*, 2000; Bischof *et al*, 2002; de Stanchina *et al*, 2004). The pro-proliferative function of TBX2 is further underscored by our results obtained in human cells depleted for TBX2, which rapidly enter senescence. Taken together, our work describes

 ©2012 European Molecular Biology Organization

an autoregulatory loop, leading to a run-away senescence outcome and thus adds another level of complexity for PML function in the weaving of a tumour-suppressive network and highlights a paramount role for TBX2 in cell proliferation.

Materials and methods

Cell culture and senescence analysis

$PML^{+/+}$ and $PML^{-/-}$ MEFs were isolated from E12.5 embryos by standard procedures. WI38 primary human lung fibroblasts, MEFs, NIH3T3, U2OS and MCF-7 cells were grown in DMEM supplemented with 10% fetal bovine serum (FBS) and penicillin/streptomycin. All cells were maintained at 37°C under an atmosphere containing 3% (for fibroblasts) or 21% (for other cell lines) O_2. Cellular senescence was monitored by counting PDs, immunolabelling of Ki67 proliferation marker and staining for senescence-associated β-galactosidase (SABG) activity as described previously (Bischof *et al*, 2006). Quiescence was induced by serum starvation using DMEM supplemented with 0.2% FBS for consecutive 4 days. Replicative senescent cells were generated by proliferative exhaustion and were used for experiments when cell cultures went through $\leqslant$1 PD per 2 weeks, were $\geqslant$80% positive for SABG staining and Ki-67 negative.

Plasmids, infection, transfection and reporter assays

$pBABE^{Puro}$-PML (-I and -V), $pDON^{Neo}$-TBX2 (wild type, RD1: Δ501–618 mutant and TB: R122, R123E mutant), $pDON^{Neo}$-TBX3, $pBABE^{Puro}$-Ras^{V12}, $pLNCX^{Neo}$-ER:Ras^{V12}, pLXSN-IE1, pLXSN-E7, pLXSN-E7Δ21−24, pcDNA3.1-TBX2 (WT and RD), pcDNA3.1-TBX3 and CMV-β-galactosidase plasmids have been published (Bischof *et al*, 2002, 2006) or were kind gifts of M van Lohuizen (TBX2), MA Buendia (TBX3) or J Gil ($pLNCX^{Neo}$-ER:Ras^{V12}). FLAG–PML-II, -III, -IV and PML-I were cloned in pcDNA3.1. A TBX2 promoter luciferase-reporter construct was generated by cloning from human genomic DNA a 1314-bp TBX2 promoter fragment (from −1314 to +1 relative to the TBX2 translational start site) into a luciferase-reporter plasmid. Lentiviral pLKO.1-shTBX2 vectors TRCN0000014825 (shTBX2-1) and TRCN0000014826 (shTBX2-2) as well as pLKO.1-shControl (shC) SHC002 were purchased from SIGMA and used according to the manufacturer's instructions. Infection of fibroblasts by retrovirus-mediated gene transfer was performed using Phoenix packaging cells as previously described (Bischof *et al*, 2002). At 24 h post-infection, cells were selected with 4 μg/ml puromycin or 400 μg/ml G418 (neomycin). Day 0 was defined as the time when all non-infected cells were dead after pharmaceutical selection (2 days of puromycin treatment or 10 days of G418 treatment). To activate ER:Ras^{V12}, infected cells were treated with 100 nM 4OHT or EtOH. Transfections of plasmids were performed with Lipofectamine and Plus reagents (Invitrogen). Luciferase and β-galactosidase activities were measured using the Luciferase-reporter assay system (Promega) and the Galacto-star (Tropix) luminescent assay kits according to the manufacturer's instructions. Luciferase activities were normalized with β-galactosidase activities.

Protein extraction and co-immunoprecipitation

Cells were washed in PBS supplemented with 10 mM *N*-ethylmaleimide (NEM; Sigma) and, for direct western blots, were scraped and lysed in sodium dodecyl sulphate (SDS) sample buffer containing 2% SDS. For co-immunoprecipitation of overexpressed proteins, cells were scraped in PBS/NEM and lysed in Chris buffer containing 50 mM Tris pH 8.0, 0.5% Nonidet P-40 (NP-40), 200 mM NaCl, 0.1 mM EDTA, 10% glycerol, 10 mM NEM and protease inhibitors (Complete EDTA free, Roche). Total cell lysates were then incubated for 2 h at 4°C with the appropriate antibody. For co-immunoprecipitation of endogenous proteins, cells were scraped in PBS/NEM and lysed in RIPA buffer (50 mM Tris pH 8.0, 1% Triton X-100, 150 mM NaCl, 0.5% sodium deoxycholate, 0.1% SDS, 1 mM EDTA, 10 mM NEM and protease inhibitors). Total cell lysates were then incubated three times for 4 h at 4°C with the appropriate antibody. Immune complexes were collected by incubation for 2 h at 4°C with Protein G plus/Protein A agarose (Calbiochem) and washed three times in lysis buffer.

Immunoblotting, immunofluorescence and antibodies

Whole-cell lysates and immunoprecipitates were separated by SDS–PAGE and analysed by immunoblotting, prepared on Hybond C-extra membranes (Amersham) and revealed using CDP-Star (Tropix). Immunofluorescence was as described (Bischof *et al*, 2002). Primary antibodies used were mouse anti-human pan-PML (PG-M3; Santa Cruz), mouse anti-mouse PML (Upstate), rabbit anti-TBX2 (Jacobs *et al*, 2000), rabbit anti-p130, rabbit anti-E2F4, goat anti-TBX3 (all from Santa Cruz), mouse anti-FLAG (M2, Sigma), mouse anti-β-actin (Sigma), mouse anti-tubulin (Calbiochem), rabbit anti-H3K27me_3, anti-H3K9me_2 and anti-H3K4me_3 (Upstate). Rabbit polyclonal antibodies recognizing human PML isoforms and the corresponding pre-immune serum were produced in-house using GST-tagged PML isoform-specific carboxy-terminal regions or peptides as antigens.

RNA isolation, affymetrix analysis, northern blot and RT–PCR analysis

Total RNA was prepared using the RNeasy RNA isolation kit (Qiagen). Transcriptome analysis using Affymetrix microarrays were performed by standard protocols at the microarray platform at IGBMC Strassbourg. Northern blot was conducted according to standard protocols using random primed probes for TBX2 and $G2a_i$. For qRT–PCR analysis, total RNA was reverse transcribed using the High Capacity cDNA Reverse Transcription kit (Applied Biosystems). cDNAs were PCR amplified using the indicated QuantiTect primers (Qiagen) and SYBR Green PCR master mix (Applied Biosystems). Real-time quantitative PCR was performed on the ABI PRISM® 7900HT Sequence Detection System (Applied Biosystems).

Chromatin immunoprecipitation

Cells were crosslinked for 15 min at 20°C by adding formaldehyde directly to the culture medium at a final concentration of 1% and ChIP was carried out as previously described (Bischof *et al*, 2006). ChIPed DNA was analysed by PCR or qPCR using TaKaRa LA Taq with GC buffer and the following primers: 5′-CCTGCG GAGAACTCCAGGTTC-3′ and 5′-GAAAGAGACAGCAGGCACTGG-3′ (primer pair 1), 5′-CCGCCCACCGGCCTCGCTTTC-3′ and 5′-GAAA GGGCCTGAGGCGAGGGG-3′ (primer pair 2), 5′-CTTCCCCAAGG CCCCGGGACC-3′ and 5′-GACAGCTCAGGCCAAGCTCCG-3′ (primer pair 3), 5′-CTTCCGACACCTTCTCCCAGG-3′ and 5′-CTGGGCCGGG CTGAGCTGGCC-3′ (primer pair 4), 5′-CTAACCAGTCGCGCGTGGTC C-3′ and 5′-CTCTCATCGGGACATCCGGCC-3′ (primer pair 5) for TBX2 promoter and 5′-GGACCTGACCTGCCGTCTAGAA-3′ and 5′-GGTGT CGCTGTTGAAGTCAGAG-3′ for GAPDH promoter. The following primers were used for the CDC6 promoter analysis: 5′-AGG GGA ACC ACA TCT TGA CAC-3′ and 5′-AAC GGG GGA GGG AAT CTA CAT C-3′. Real-time qPCR was performed on the ABI PRISM 7900HT Sequence Detection System (Applied Biosystems) using the SYBR Green PCR master mix (Applied Biosystems).

Supplementary data

Supplementary data are available at *The EMBO Journal* Online (http://www.embojournal.org).

Acknowledgements

We acknowledge all members of the laboratory for helpful discussions. This work was supported by grants from EEC 6th FP, LNCC (Equipe labellisée), AICR, ANR and ARC. OB is a CNRS fellow. NM was supported by MRT, MDD by OdysseyRe and MB by ARC.

Author contributions: OB and AD conceived the project. OB, NM, MB and AD designed and performed the experiments. KN and OB produced PML isoform-specific antibodies, MD produced $PML^{-/-}$ MEFs and MvL provided technical assistance, discussion and valuable reagents. OB, AD, NM and MB analysed data. OB and AD wrote manuscript.

Conflict of interest

The authors declare that they have no conflict of interest.

©2012 European Molecular Biology Organization

References

Abrahams A, Parker MI, Prince S (2010) The T-box transcription factor Tbx2: its role in development and possible implication in cancer. *IUBMB Life* **62:** 92–102

Agulnik SI, Bollag RJ, Silver LM (1995) Conservation of the T-box gene family from Mus musculus to Caenorhabditis elegans. *Genomics* **25:** 214–219

Bernardi R, Pandolfi PP (2007) Structure, dynamics and functions of promyelocytic leukaemia nuclear bodies. *Nat Rev Mol Cell Biol* **8:** 1006–1016

Bischof O, Kirsh O, Pearson M, Itahana K, Pelicci PG, Dejean A (2002) Deconstructing PML-induced premature senescence. *EMBO J* **21:** 3358–3369

Bischof O, Nacerddine K, Dejean A (2005) Human papillomavirus oncoprotein E7 targets the promyelocytic leukemia protein and circumvents cellular senescence via the Rb and p53 tumor suppressor pathways. *Mol Cell Biol* **25:** 1013–1024

Bischof O, Schwamborn K, Martin N, Werner A, Sustmann C, Grosschedl R, Dejean A (2006) The E3 SUMO ligase PIASy is a regulator of cellular senescence and apoptosis. *Mol Cell* **22:** 783–794

Block GJ, Eskiw CH, Dellaire G, Bazett-Jones DP (2006) Transcriptional regulation is affected by subnuclear targeting of reporter plasmids to PML nuclear bodies. *Mol Cell Biol* **26:** 8814–8825

Cam H, Balciunaite E, Blais A, Spektor A, Scarpulla RC, Young R, Kluger Y, Dynlacht BD (2004) A common set of gene regulatory networks links metabolism and growth inhibition. *Mol Cell* **16:** 399–411

Campisi J, d'Adda di Fagagna F (2007) Cellular senescence: when bad things happen to good cells. *Nat Rev Mol Cell Biol* **8:** 729–740

Carreira S, Liu B, Goding CR (2000) The gene encoding the T-box factor Tbx2 is a target for the microphthalmia-associated transcription factor in melanocytes. *J Biol Chem* **275:** 21920–21927

Chen Z, Trotman LC, Shaffer D, Lin HK, Dotan ZA, Niki M, Koutcher JA, Scher HI, Ludwig T, Gerald W, Cordon-Cardo C, Pandolfi PP (2005) Crucial role of p53-dependent cellular senescence in suppression of Pten-deficient tumorigenesis. *Nature* **436:** 725–730

Chicas A, Wang X, Zhang C, McCurrach M, Zhao Z, Mert O, Dickins RA, Narita M, Zhang M, Lowe SW (2010) Dissecting the unique role of the retinoblastoma tumor suppressor during cellular senescence. *Cancer Cell* **17:** 376–387

Courtois-Cox S, Genther Williams SM, Reczek EE, Johnson BW, McGillicuddy LT, Johannessen CM, Hollstein PE, MacCollin M, Cichowski K (2006) A negative feedback signaling network underlies oncogene-induced senescence. *Cancer Cell* **10:** 459–472

Davis E, Teng H, Bilican B, Parker MI, Liu B, Carriera S, Goding CR, Prince S (2008) Ectopic Tbx2 expression results in polyploidy and cisplatin resistance. *Oncogene* **27:** 976–984

de Stanchina E, Querido E, Narita M, Davuluri RV, Pandolfi PP, Ferbeyre G, Lowe SW (2004) PML is a direct p53 target that modulates p53 effector functions. *Mol Cell* **13:** 523–535

Dyson N (1998) The regulation of E2F by pRB-family proteins. *Genes Dev* **12:** 2245–2262

Everett RD, Chelbi-Alix MK (2007) PML and PML nuclear bodies: implications in antiviral defence. *Biochimie* **89:** 819–830

Ferbeyre G, de Stanchina E, Querido E, Baptiste N, Prives C, Lowe SW (2000) PML is induced by oncogenic ras and promotes premature senescence. *Genes Dev* **14:** 2015–2027

Frolov MV, Dyson NJ (2004) Molecular mechanisms of E2F-dependent activation and pRB-mediated repression. *J Cell Sci* **117**(Part 11)**:** 2173–2181

Gabai VL, Yaglom JA, Waldman T, Sherman MY (2009) Heat shock protein Hsp72 controls oncogene-induced senescence pathways in cancer cells. *Mol Cell Biol* **29:** 559–569

Gurrieri C, Capodieci P, Bernardi R, Scaglioni PP, Nafa K, Rush LJ, Verbel DA, Cordon-Cardo C, Pandolfi PP (2004a) Loss of the tumor suppressor PML in human cancers of multiple histologic origins. *J Natl Cancer Inst* **96:** 269–279

Gurrieri C, Nafa K, Merghoub T, Bernardi R, Capodieci P, Biondi A, Nimer S, Douer D, Cordon-Cardo C, Gallagher R, Pandolfi PP (2004b) Mutations of the PML tumor suppressor gene in acute promyelocytic leukemia. *Blood* **103:** 2358–2362

He M, Wen L, Campbell CE, Wu JY, Rao Y (1999) Transcription repression by Xenopus ET and its human ortholog TBX3, a gene involved in ulnar-mammary syndrome. *Proc Natl Acad Sci USA* **96:** 10212–10217

Helmbold H, Deppert W, Bohn W (2006) Regulation of cellular senescence by Rb2/p130. *Oncogene* **25:** 5257–5262

Ismail A, Bateman A (2009) Expression of TBX2 promotes anchorage-independent growth and survival in the p53-negative SW13 adrenocortical carcinoma. *Cancer Lett* **278:** 230–240

Jackson JG, Pereira-Smith OM (2006) Primary and compensatory roles for RB family members at cell cycle gene promoters that are deacetylated and downregulated in doxorubicin-induced senescence of breast cancer cells. *Mol Cell Biol* **26:** 2501–2510

Jacobs JJ, Keblusek P, Robanus-Maandag E, Kristel P, Lingbeek M, Nederlof PM, van Welsem T, van de Vijver MJ, Koh EY, Daley GQ, van Lohuizen M (2000) Senescence bypass screen identifies TBX2, which represses Cdkn2a (p19(ARF)) and is amplified in a subset of human breast cancers. *Nat Genet* **26:** 291–299

Jacobs JJ, Kieboom K, Marino S, DePinho RA, van Lohuizen M (1999) The oncogene and Polycomb-group gene bmi-1 regulates cell proliferation and senescence through the ink4a locus. *Nature* **397:** 164–168

Jensen K, Shiels C, Freemont PS (2001) PML protein isoforms and the RBCC/TRIM motif. *Oncogene* **20:** 7223–7233

Jenuwein T (2006) The epigenetic magic of histone lysine methylation. *FEBS J* **273:** 3121–3135

Kumar PP, Bischof O, Purbey PK, Notani D, Urlaub H, Dejean A, Galande S (2007) Functional interaction between PML and SATB1 regulates chromatin-loop architecture and transcription of the MHC class I locus. *Nat Cell Biol* **9:** 45–56

Lin AW, Barradas M, Stone JC, van Aelst L, Serrano M, Lowe SW (1998) Premature senescence involving p53 and p16 is activated in response to constitutive MEK/MAPK mitogenic signaling. *Genes Dev* **12:** 3008–3019

Lingbeek ME, Jacobs JJ, van Lohuizen M (2002) The T-box repressors TBX2 and TBX3 specifically regulate the tumor suppressor gene p14ARF via a variant T-site in the initiator. *J Biol Chem* **277:** 26120–26127

Mallette FA, Goumard S, Gaumont-Leclerc MF, Moiseeva O, Ferbeyre G (2004) Human fibroblasts require the Rb family of tumor suppressors, but not p53, for PML-induced senescence. *Oncogene* **23:** 91–99

Mann KK, Shao W, Miller Jr WH (2001) The biology of acute promyelocytic leukemia. *Curr Oncol Rep* **3:** 209–216

Minucci S, Nervi C, Lo Coco F, Pelicci PG (2001) Histone deacetylases: a common molecular target for differentiation treatment of acute myeloid leukemias? *Oncogene* **20:** 3110–3115

Narita M, Nunez S, Heard E, Lin AW, Hearn SA, Spector DL, Hannon GJ, Lowe SW (2003) Rb-mediated heterochromatin formation and silencing of E2F target genes during cellular senescence. *Cell* **113:** 703–716

Pearson M, Carbone R, Sebastiani C, Cioce M, Fagioli M, Saito S, Higashimoto Y, Appella E, Minucci S, Pandolfi PP, Pelicci PG (2000) PML regulates p53 acetylation and premature senescence induced by oncogenic Ras. *Nature* **406:** 207–210

Prince S, Carreira S, Vance KW, Abrahams A, Goding CR (2004) Tbx2 directly represses the expression of the p21(WAF1) cyclin-dependent kinase inhibitor. *Cancer Res* **64:** 1669–1674

Serrano M, Lin AW, McCurrach ME, Beach D, Lowe SW (1997) Oncogenic ras provokes premature cell senescence associated with accumulation of p53 and p16INK4a. *Cell* **88:** 593–602

Takahashi Y, Rayman JB, Dynlacht BD (2000) Analysis of promoter binding by the E2F and pRB families *in vivo*: distinct E2F proteins mediate activation and repression. *Genes Dev* **14:** 804–816

Tarutani M, Cai T, Dajee M, Khavari PA (2003) Inducible activation of Ras and Raf in adult epidermis. *Cancer Res* **63:** 319–323

Teng H, Davis E, Abrahams A, Mowla S, Parker MI, Prince S (2007) A role for Tbx2 in the regulation of the alpha2(1) collagen gene in human fibroblasts. *J Cell Biochem* **102:** 618–625

Trimarchi JM, Lees JA (2002) Sibling rivalry in the E2F family. *Nat Rev Mol Cell Biol* **3:** 11–20

Vance KW, Carreira S, Brosch G, Goding CR (2005) Tbx2 is overexpressed and plays an important role in maintaining proliferation and suppression of senescence in melanomas. *Cancer Res* **65:** 2260–2268

 ©2012 European Molecular Biology Organization

Vernier M, Bourdeau V, Gaumont-Leclerc MF, Moiseeva O, Begin V, Saad F, Mes-Masson AM, Ferbeyre G (2011) Regulation of E2Fs and senescence by PML nuclear bodies. *Genes Dev* **25:** 41–50

Villa R, Pasini D, Gutierrez A, Morey L, Occhionorelli M, Vire E, Nomdedeu JF, Jenuwein T, Pelicci PG, Minucci S, Fuks F, Helin K, Di Croce L (2007) Role of the polycomb repressive complex 2 in acute promyelocytic leukemia. *Cancer Cell* **11:** 513–525

Wang J, Shiels C, Sasieni P, Wu PJ, Islam SA, Freemont PS, Sheer D (2004) Promyelocytic leukemia nuclear bodies associate with transcriptionally active genomic regions. *J Cell Biol* **164:** 515–526

Wang ZG, Delva L, Gaboli M, Rivi R, Giorgio M, Cordon-Cardo C, Grosveld F, Pandolfi PP (1998) Role of PML in cell growth and the retinoic acid pathway. *Science* **279:** 1547–1551

Xu ZX, Zhao RX, Ding T, Tran TT, Zhang W, Pandolfi PP, Chang KS (2004) Promyelocytic leukemia protein 4 induces apoptosis by inhibition of survivin expression. *J Biol Chem* **279:** 1838–1844

Zhong S, Salomoni P, Pandolfi PP (2000) The transcriptional role of PML and the nuclear body. *Nat Cell Biol* **2:** E85–E90

©2012 European Molecular Biology Organization